Leuzzi et al.

WRNIP1 protects stalled forks from degradation and promotes fork restart after replication stress

- Appendix-

Table of contents:

APPENDIX SUPPLEMENTARY MATHERIALS AND METHODS

Chemicals

Chemicals used were commercially obtained for the replication stress-inducing drugs, hydroxyurea and aphidicolin (Sigma-Aldrich), the inibitor of RAD51 activity (B02; Calbiochem), the inibitor of MRE11 exonuclease activity (Mirin; Calbiochem), and the proteasome inhibitor (MG132; Sigma-Aldrich).

Site-directed mutagenesis and cloning

Site-directed mutagenesis of the WRNIP1 full-lenght cDNA (Open Biosystems) was performed on the pCMV-FLAGWRNIP1 plasmid that contains the wild-type ORF sequence of WRNIP1. Substitution of Thr 294 to Ala in pCMV-FLAGWRNIP1 was introduced by the Quick-change XL kit (Stratagene) using mutagenic primer pairs designed, according to the manufacturer's instructions. Each mutated plasmid was verified by full sequencing of the WRNIP1 ORF.

Plasmids and RNA interference

Plasmid expressing the wild-type human RAD51 (TU/T7-RAD51) was kindly provided by Maria Spies (University of Iowa, USA). The plasmid was transfected using the Neon^{TM} Transfection System Kit (Invitrogen), according to the manufacturer's instructions.

WRNIP1, BRCA2, MRE11, RAD51 and FBH1 genetic knockdown experiments were performed by Interferin (Polyplus), according to the manufacturer's instructions. siRNAs were used at 10 nM. As a control, a siRNA duplex directed against GFP was used. All depletions were achieved using siRNAs (QIAGEN) targeting the 3'UTR regions of the following human proteins: WRNIP1 (5'-ATGAATTAATGTTATAAGG-3'), BRCA2 (5'-CAGGACACAATTACAACTAAA-3'), MRE11 (5'-AAGGGTTATTTGAGCAAGTAA-3'), RAD51 (5'-CAGGATAAAGCTTCCGGGA-3') and FBH1 (5'-TAGGGCGGAAGTACCAGTCAA-3'). Depletion was confirmed by Western blot using the relevant antibodies (*see below*).

Co-immunoprecipitation, cell fractionation and Western blot analysis

Immunoprecipitation and chromatin fractionation experiments were performed as previously described (Basile *et al*, 2014). Briefly, for co-immunoprecipitation (co-IP)

experiments, exponential growing HEK293T cells were cultured overnight at a density of 2.5×10^6 per 150 mm Petri dish, and treated or not as indicated. After treatment, cells were collected and centrifuged. The cell pellets were resuspended in lysis co-IP buffer (1% Triton X-100, 0.5% Na-dehoxycolate, 150 mM NaCl, 1 mM EGTA, 20 mM Tris/HCl pH 8.0), freshly supplemented with protease inhibitor cocktail (Thermo Scientific), and sonicated on ice. After centrifugation, for each IP sample, lysate was incubated with 20 µl anti-FLAG M2 magnetic beads (Sigma-Aldrich) at 4°C overnight. The IP reaction was washed three times with the co-IP buffer, incubated in 2× sample loading buffer (100 mM Tris/HCl pH 6.8, 100 mM DTT, 4% SDS, 0.2% bromophenol blue and 20% glycerol) for 30 min at 90°C, then subjected to Western blot as described below.

Analysis of the distribution of proteins in the chromatin fraction was carried out by a standard protocol of chromatin fractionation (Méndez & Stillman, 2000). Briefly, 1.5×10^7 cells were harvested using a cell scraper, centrifuged (2 min, 1.300 × g, 4°C), and then pellet was washed twice with PBS (2 min, 1.300 × g, 4°C). Cell pellet were resuspended in buffer A (10 mM HEPES pH 7.9, 10 mM KCl, 1.5 mM $MgCl_2$, 0.34 M sucrose, 10% glycerol, 1 mM DTT, supplemented with protease inhibitor cocktail). Triton X-100 (0.1%) was added, and the cells were incubated for 5 min on ice. Nuclei were collected in pellet by centrifugation (4 min, 1.300 × g, 4°C). The supernatant was discarded, nuclei washed once in buffer A, and then lysed in buffer B (3 mM EDTA, 0.2 mM EGTA, 1 mM DTT, supplemented with protease inhibitor cocktail). Insoluble chromatin was collected by centrifugation (4 min, 1.700 × g, 4°C), washed once in buffer B, and centrifuged again under the same conditions. The final chromatin pellet was resuspended in 2× sample loading buffer (100 mM Tris/HCl pH 6.8, 100 mM DTT, 4% SDS, 0.2% bromophenol blue and 20% glycerol), sonicated on ice, and boiled for 30 min at 90°C, then subjected to Western blot as reported below.

The proteins were resolved on a 4 - 15% Mini-Protean TGX precast polyacrylamide gels (Bio-Rad), and transferred onto nitrocellulose membrane using the Trans-Blot Turbo Transfer System (Bio-Rad). The membranes were blocked using 5% NFDM in TBST (50 mM Tris/HCl pH 8, 150 mM NaCl, 0.1% Tween-20), and incubated with primary antibody for 2 h at RT. The primary antibodies used for WB were: rabbit-polyclonal anti-WRNIP1 (Novus Biologicals, 1:2000), mouse-monoclonal anti-FLAG (Sigma-Aldrich, 1:1000), mouse-polyclonal anti-GAPDH (Millipore, 1:5000), rabbit-polyclonal anti-RAD51 (Santa Cruz Biotechnology, 1:500), rabbit-polyclonal anti-LAMIN B1 (Abcam, 1:10000), rabbit-

polyclonal anti-BRCA2 (Bethyl, 1:1000), mouse-monoclonal anti-MRE11 (Novus Biological, 1:2000) and mouse-monoclonal anti-FBH1 (Abcam, 1:200).
The membranes were incubated with horseradish peroxidase-conjugated goat specie-specific secondary antibodies (Santa Cruz Biotechnology, 1:20000), for 1 h at RT. Visualisation of the signal was accomplished using Super Signal West Dura substrate (Thermo Fisher Scientific), and developed by chemiluminescence and imaged using Chemidoc (GE healthcare LAS 4000).

Neutral and alkaline Comet assay

The occurrence of DNA double-strand breaks was evaluated by neutral Comet assay as described (Murfuni *et al*, 2012). Cell DNA was stained with a fluorescent dye GelRed (Biotium), and examined at 40× magnification with an Olympus fluorescence microscope. Slides were analyzed by a computerized image analysis system (Comet IV, Perceptive UK). To assess the amount of DNA damage, computer-generated tail moment values (tail length × fraction of total DNA in the tail) were used. A minimum of 200 cells was analyzed for each experimental point. Apoptotic cells (smaller comet head and extremely larger comet tail) were excluded from the analysis to avoid artificial enhancement of the tail moment.
DNA breakage induction was examined by alkaline Comet assay (single-cell gel electrophoresis) in denaturing conditions as described (Pichierri *et al*, 2001). Cell DNA was stained with a fluorescent dye GelRed (Biotium), and examined at 40× magnification with an Olympus fluorescence microscope. Slides were analyzed as described above.

Immunofluorescence

Immunofluorescence analysis was performed as previously described (Murfuni *et al*, 2012). Briefly, exponential growing cells were seeded onto Petri dish, then treated (or mock-treated) as indicated, fixed in 2% formaldehyde for 10 min, and permeabilized using 0.4% Triton X-100 for 10 min before being incubated with 10% FBS for 1 h. After blocking, for γ-H2AX, BRCA2 and RAD51 detection, cells were incubated with the following primary antibodies: mouse-monoclonal anti-γ-H2AX (Millipore, 1:1000), rabbit-polyclonal anti-BRCA2 (Bethyl, 1:1000) or rabbit-polyclonal anti-RAD51 (Santa Cruz Biotechnology, 1:500), respectively. Cells were washed twice with PBS, and then incubated with the following secondary antibodies: goat anti-mouse Alexa Fluor 488 or goat anti-rabbit Alexa

Fluor 594 (Molecular Probes, 1:200). The incubation with antibodies were accomplished in a humidified chamber for 1 h at RT. DNA was counterstained with 0.5 µg/ml DAPI (blue florescence). Images were acquired randomly using Eclipse 80i Nikon Fluorescence Microscope, equipped with a VideoConfocal (ViCo) system. For each time point, at least 200 nuclei were examined, and foci were scored at a 60× magnification. Only nuclei showing more than five bright foci were counted as positive. Parallel samples incubated with either the appropriate normal serum or only with the secondary antibody confirmed that the observed fluorescence pattern was not attributable to artefacts.

To detect parental-strand ssDNA, cells were pre-labelled for 24 h with 10 µM IdU (Sigma-Aldrich), washed in drug-free medium, then treated with 4 mM HU for 4 h. To detect nascent-strand ssDNA, cells were pre-labelled for 20 min with 10 µM IdU (Sigma-Aldrich), then 4 mM HU was added for 4 h. Next, cells were washed with PBS, permeabilized with 0.5% Triton X-100 for 10 min at 4°C, fixed with 3% formaldehyde/ 2% sucrose solution for 10 min, and then blocked in 3% BSA/PBS for 15 min as previously described (Couch *et al*, 2013). Fixed cells were then incubated with anti-IdU antibody (mouse-monoclonal anti-BrdU/IdU; clone b44 Becton Dickinson, 1:10). Cells were washed twice with PBS, and then incubated with goat anti-mouse Alexa Fluor 488 (Molecular Probes, 1:200). The secondary antibodies were: goat anti-mouse Alexa Fluor 488 or goat anti-rabbit Alexa Fluor 594 (Molecular Probes, 1:200). The incubation with antibodies was accomplished in a humidified chamber for 1 h at RT. DNA was counterstained with 0.5 µg/ml DAPI. Images were acquired as described above.

LIVE/DEAD staining

Viability was evaluated by the fluorescence-based assay the LIVE/DEAD Cell Double Staining Kit (Sigma-Aldrich), according to the manufacturer's instructions. LIVE/DEAD assay is a short-term viability assay that allows direct evaluation of the number of live cells, stained in green with calcein-AM, and that of dead cells, stained in red with propidium iodide (PI). Since both calcein and PI-DNA can be excited with 490 nm light, simultaneous monitoring of live and dead cells is possible with a fluorescence microscope. Cell number was counted in randomly chosen fields and expressed as percent of dead cells (number of red nuclear stained cells/total cell number). For each time point, at least 1000 cells were counted.

Chromosomal aberration analysis

Cells for metaphase preparations were collected according to standard procedure and as previously reported (Pirzio *et al*, 2008). Cell suspension was dropped onto cold, wet slides to make chromosome preparations. The slides were air dried overnight, then for each condition of treatment, the number of breaks and gaps was observed on Giemsa-stained metaphases. For each time point, at least 50 chromosomes were examined by two independent investigators and chromosomal damage was scored at 100× magnification with an Olympus fluorescence microscope.

Cell cycle analysis by flow cytometry

Flow cytometric cell cycle analysis was performed as follow: cell cultures were treated with 4 mM HU for 4h, then harvested by trypsinization. After centrifugation, collected cells were washed twice in PBS/BSA, then fixed in 50% cold methanol. After an overnight incubation at -20°C, cells were centrifuged and washed twice in PBS/BSA. Finally, pellets were resuspended, and cells stained with PI solution (propidium iodide 20 µg/ml) for 30 min at 4°C in the dark. Samples were analyzed by flow cytometry, and data analysis was conducted with CellQuest software.

APPENDIX SUPPLEMENTARY LEGENDS TO FIGURES

Fig S1. Analysis of replication dynamics in WRNIP1-deficient and mutant cells

(**A**) Experimental scheme of pulse-labelling of DNA fibers in wild-type (shWRNIP1^{WT}), WRNIP1-deficient (shWRNIP1) and mutant (shWRNIP1^{T294A}) cells. Cells were pulse-labelled with CldU, treated with 4mM HU and then subjected to a pulse-labelling with IdU. (**B**) Graphs show the percentage of green (IdU) tracts (new origins), red-green-red (IdU-CldU-IdU) contiguous tracts (termination events) or multiple CldU and IdU labels (interspersed fibers) in the cells. Mean shown, n = 3. Error bars represent standard error. (ns, not significant; Student's t test).

Fig S2. WRNIP1-deficient cells shows nascent DNA strand degradation after Aph-induced replication stress

(**A**) Scheme of DNA fiber tract analysis in wild-type (shWRNIP1^{WT}) and WRNIP1-deficient (shWRNIP1) cells. Cells were pulse-labelled with IdU and treated or not with 10 μM Aph. (**B**) Representative IdU tract length distributions in all cell lines under unperturbed conditions (left graph) or after Aph treatment (right graph). Median tract lengths are given in parentheses. See also Table S1 and S2 for details on the data sets and statistical test.

Fig S3. WRNIP1 interference in HEK293T cells results in nascent DNA strand degradation after replication stress

(**A**) Experimental scheme of pulse-labelling of DNA fibers in HEK293T cells transfected with control siRNA (HEK293T^{siCtrl}) or *WRNIP1* siRNA (HEK293T^{siWRNIP1}), and 48 h thereafter labelled with IdU. Next, cells were treated or not with 4 mM HU. (**B**) Representative IdU tract length distributions in HEK293T^{siCtrl} or HEK293T^{siWRNIP1} cells under unperturbed conditions (left graph) or after HU (right graph). Median tract lengths are given in parentheses. Representative DNA fiber images are reported. Scale bars, 10 μm. Western blot shows the expression of the WRNIP1 protein in the cells. The membrane was probed with an anti-WRNIP1. GAPDH was used as a loading control.

Fig S4. MRE11 interference in WRNIP1-deficient cells results in avoidance of nascent DNA strand degradation after replication stress

(**A**) Scheme of DNA fiber tract analysis in WRNIP1-deficient (shWRNIP1) cells. Cells were transfected with control siRNA (siCtrl) or *MRE11* siRNA (siMRE11), and 48 h thereafter labelled with IdU. Next, cells were treated or not with 4 mM HU. (**B**) Representative IdU tract length distributions in shWRNIP1 (shWRNIP1^{siCtrl}) cells or shWRNIP1 cells, in which MRE11 was depleted (shWRNIP1^{siMRE11}), treated or not with 4 mM HU. Median tract lengths are given in parentheses. See Tables S1 and S2 for details on the data sets and statistical test. Western blot shows MRE11 depletion in shWRNIP1 cells. The membrane was probed with an anti-MRE11. GAPDH was used as a loading control.

Fig S5. MRE11 depletion reduces ssDNA accumulation at parental-strand in WRNIP1-deficient cells

(**A**) Scheme of parental ssDNA assay. Wild-type (shWRNIP1^{WT}) and WRNIP1-deficient (shWRNIP1) cells were transfected with control siRNA (siCtrl) or *MRE11* siRNA (siMRE11), and 48 h afterward labelled with IdU for 24 h as indicated. Cells were washed

and left to recover for 2 h, then treated with 4 mM HU. After treatment, cells were fixed and stained with an anti-IdU antibody without denaturing the DNA to specifically detect ssDNA at parental-strand. (**B**) Dot plot shows IdU intensity per nucleus. The intensity of the anti-IdU immunofluorescence was measured in at least 50 nuclei from two independent experiments. Horizontal black lines represent the mean ± SE. Error bars represent standard error (ns, not significant; ****, p<0.0001; two-tailed Student's t test). Western blot shows MRE11 depletion in shWRNIP1^{WT} and shWRNIP1 cells. The membrane was probed with an anti-MRE11. GAPDH was used as a loading control.

Fig S6. Analysis of nascent ssDNA accumulation in WRNIP1-deficient cells

(**A**) Experimental design of ssDNA assay is reported. Wild-type (shWRNIP1^{WT}) and WRNIP1-deficient (shWRNIP1) cells were short-labelled with IdU, washed and treated or not with 4 mM HU for 4 h. After that, cells were fixed and stained with an anti-IdU antibody without denaturing the DNA to specifically detect nascent ssDNA. (**B**) Dot plot shows IdU intensity per nucleus. Horizontal black lines represent the mean ± SE. Error bars represent standard error (ns, not significant; two-tailed Student's t test). Representative images are shown. DNA was counterstained with DAPI (blue).

Fig S7. Immunostaining analysis of RAD51

Wild-type (shWRNIP1^{WT}) or WRNIP1-deficient (shWRNIP1) cells were untreated or treated with 4 mM HU for 4 h, and then processed for immunofluorescence analysis with a specific anti-RAD51 antibody. The graph shows the percentage of cells with RAD51-foci. Representative images of cells stained for RAD51 are given. Nuclei were counterstained with DAPI (blue).

Fig S8. MG132 treatment does not accumulate RAD51 on chromatin after fork stalling

Analysis of chromatin binding of RAD51 in wild-type (shWRNIP1^{WT}) or WRNIP1-deficient (shWRNIP1) cells. Chromatin fractions of cells, treated or not with HU and proteasome inhibitor MG132 at the indicated times, were analysed by immunoblotting. The membrane was probed with an anti- anti-RAD51 antibody. LAMIN B1 was used as a loading for the chromatin fraction.

Fig S9. RAD51 interference in WRNIP1-deficient cells results in enhanced nascent DNA strand degradation after replication stress

(A) Scheme of DNA fiber tract analysis in wild-type (shWRNIP1^{WT}) or WRNIP1-deficient (shWRNIP1) cells. Cells were transfected with control siRNA (siCtrl) or *RAD51* siRNA (siRAD51), and 48 h thereafter labelled with IdU. Next, cells were treated or not with 4 mM HU. (**B**) Representative IdU tract length distributions in control shWRNIP1^{WT} or shWRNIP1 cells (shWRNIP1^{WT} or shWRNIP1, respectively), or cells in which RAD51 was depleted (shWRNIP1$^{WT/siRAD51}$ or shWRNIP1^{siRAD51}, respectively), treated or not with 4 mM HU. Median tract lengths are given in parentheses. See Tables S1 and S2 for details on the data sets and statistical test. Western blot shows RAD51 depletion in the cells. The membrane was probed with an anti-RAD51. LAMIN B1 was used as a loading control.

Fig S10. Loss of WRNIP1 does not affect BRCA2 relocalisation in foci after replication stress

Effect of loss of WRNIP1 on BRCA2 subnuclear relocalisation after treatment. Wild-type (shWRNIP1^{WT}) and WRNIP1-deficient (shWRNIP1) cells were treated or not with 4 mM HU for 4 h, then subjected to BRCA2 immunofluorescence. Graph shows the percentage of cells with BRCA2-positive foci after treatment. Error bars represent standard errors. (ns, not significant; two-tailed Student's t test); n =3. Representative images of cells with BRCA2 relocalised in foci after HU exposure are shown. Insets show enlarged nuclei for a better evaluation of BRCA2 relocalisation in the cells.

Fig S11 Effect of concomitant depletion of BRCA2 and FBH1 on nascent DNA strand degradation after fork stalling

(**A**) Experimental scheme of pulse-labelling of DNA fibers in wild-type (shWRNIP1^{WT}) cells. Cells were transfected with *BRCA2* siRNA alone or in combination with *FBH1* siRNA (shWRNIP1$^{WT/siBRCA2}$ and shWRNIP1$^{WT/siBRCA2/siFBH1}$, respectively), and 48 h thereafter labelled with IdU, then treated or not with 4 mM HU. (**B**) Representative IdU tract length distributions in shWRNIP1$^{WT/siBRCA2}$ or shWRNIP1$^{WT/siBRCA2/siFBH1}$ cells with or without HU treatment. Western blot shows BRCA2 and FBH1 depletion in the cells. The membrane was probed with the anti-BRCA2 and anti-FBH1 antibodies. GAPDH was used as a loading control. Median tract lengths are given in parentheses. See Tables S1 and S2 for details on the data sets and statistical test.

Fig S12 Cell cycle progression analysis

Cell cycle progression evaluated by flow cytometry. Wild-type (shWRNIP1^{WT}), WRNIP1-deficient (shWRNIP1) and mutant (shWRNIP1^{T294A}) cells were treated or not with 4 mM HU for 4 h. Cells were then harvested and stained with Propidium Iodide (PI) prior to flow-cytometric analysis. Representative DNA content profiles of the cells. Graph shows the percentage of cells distributed into G0/G1, S or G2/M phases.

Fig S13 Loss of WRNIP1 or its ATPase activity did not produce DSBs after replication fork stalling

Analysis of DSB formation evaluated by neutral Comet assay. Wild-type (shWRNIP1^{WT}), WRNIP1-deficient (shWRNIP1) or mutant (shWRNIP1^{T294A}) cells were treated with 4 mM HU for 4 h, then subjected to Comet assay. Graph shows data presented as mean tail moment ± SE from three independent experiments; n = 3. Error bars represent standard errors. (ns, not significant; two-tailed Student's t test). Representative images are shown.

Fig S14 MRE11 depletion attenuates chromosomal aberrations in WRNIP1-deficient cells after fork stalling

(**A**) Scheme of the experimental design. Wild-type (shWRNIP1^{WT}) or WRNIP1-deficient (shWRNIP1) cells were transfected with control siRNA (siCtrl) or *MRE11* siRNA (siMRE11), and 48 h thereafter treated with 4 mM HU, then left to recover for 16h in drug-free medium and metaphases collected with colcemid. Next, cells were fixed and processed as reported in "Supplemental information" section. (**B**) Analysis of chromosomal aberrations. Dot plot shows the number of chromosomal aberrations per cell. Horizontal black lines represent the mean ± SE. Error bars represent standard error (ns, not significant; *, $p < 0.1$; two-tailed Student's t test). Representative Giemsa-stained metaphases of HU-treated cells. Arrows indicate chromosomal aberrations.

APPENDIX REFERENCES

Basile G, Leuzzi G, Pichierri P & Franchitto A (2014) Checkpoint-dependent and

independent roles of the Werner syndrome protein in preserving genome integrity in response to mild replication stress. *Nucleic Acids Res.* **42:** 12628–39

Couch FB, Bansbach CE, Driscoll R, Luzwick JW, Glick GG, Bétous R, Carroll CM, Jung SY, Qin J, Cimprich KA & Cortez D (2013) ATR phosphorylates SMARCAL1 to prevent replication fork collapse. *Genes Dev.* **27:** 1610–23

Méndez J & Stillman B (2000) Chromatin association of human origin recognition complex, cdc6, and minichromosome maintenance proteins during the cell cycle: assembly of prereplication complexes in late mitosis. *Mol. Cell. Biol.* **20:** 8602–12

Murfuni I, De Santis A, Federico M, Bignami M, Pichierri P & Franchitto A (2012) Perturbed replication induced genome wide or at common fragile sites is differently managed in the absence of WRN. *Carcinogenesis* **33:** 1655–63

Pichierri P, Franchitto A, Mosesso P, Palitti F & Molecolare C (2001) Werner ' s Syndrome Protein Is Required for Correct Recovery after Replication Arrest and DNA Damage Induced in S-Phase of Cell Cycle. *Mol. Biol. Cell* **12:** 2412–2421

Pirzio LM, Pichierri P, Bignami M & Franchitto A (2008) Werner syndrome helicase activity is essential in maintaining fragile site stability. *J. Cell Biol.* **180:** 305–14

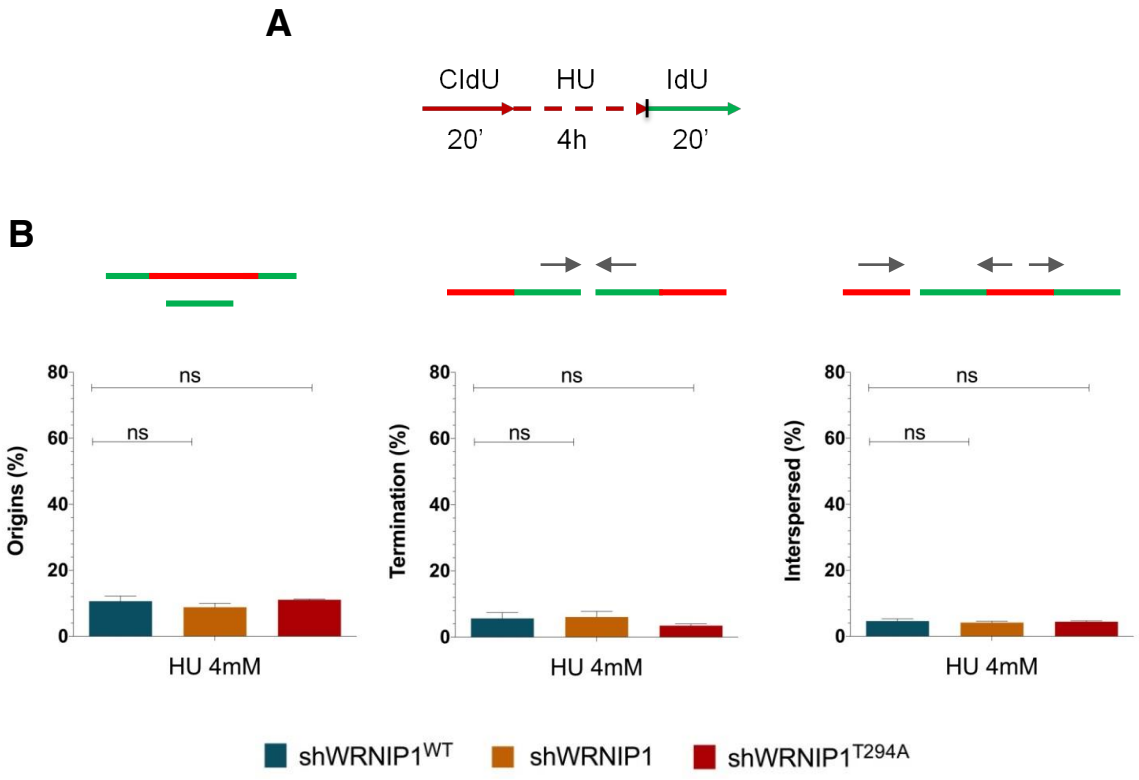

Appendix Figure S1

A

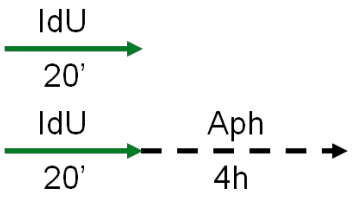

B

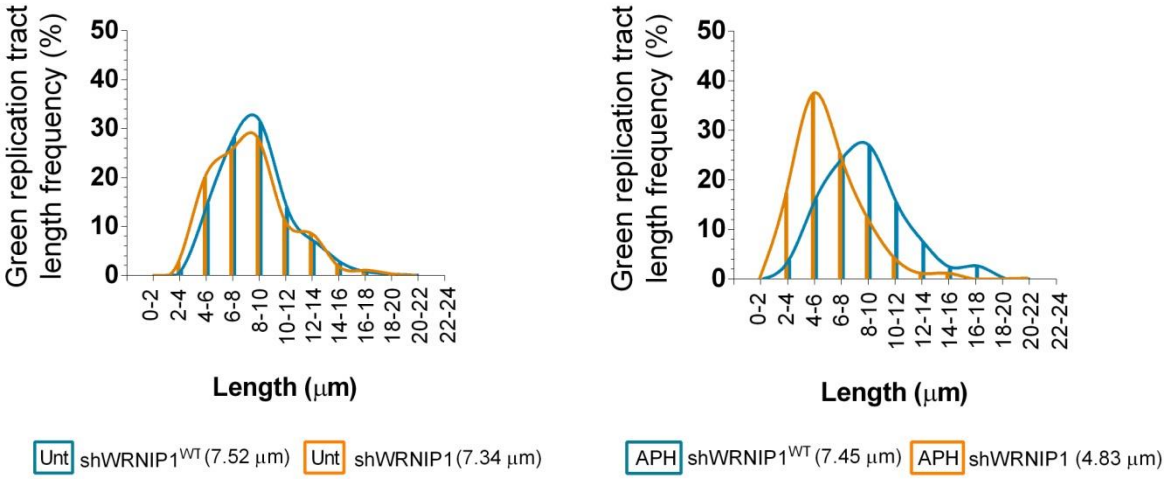

Appendix Figure S2

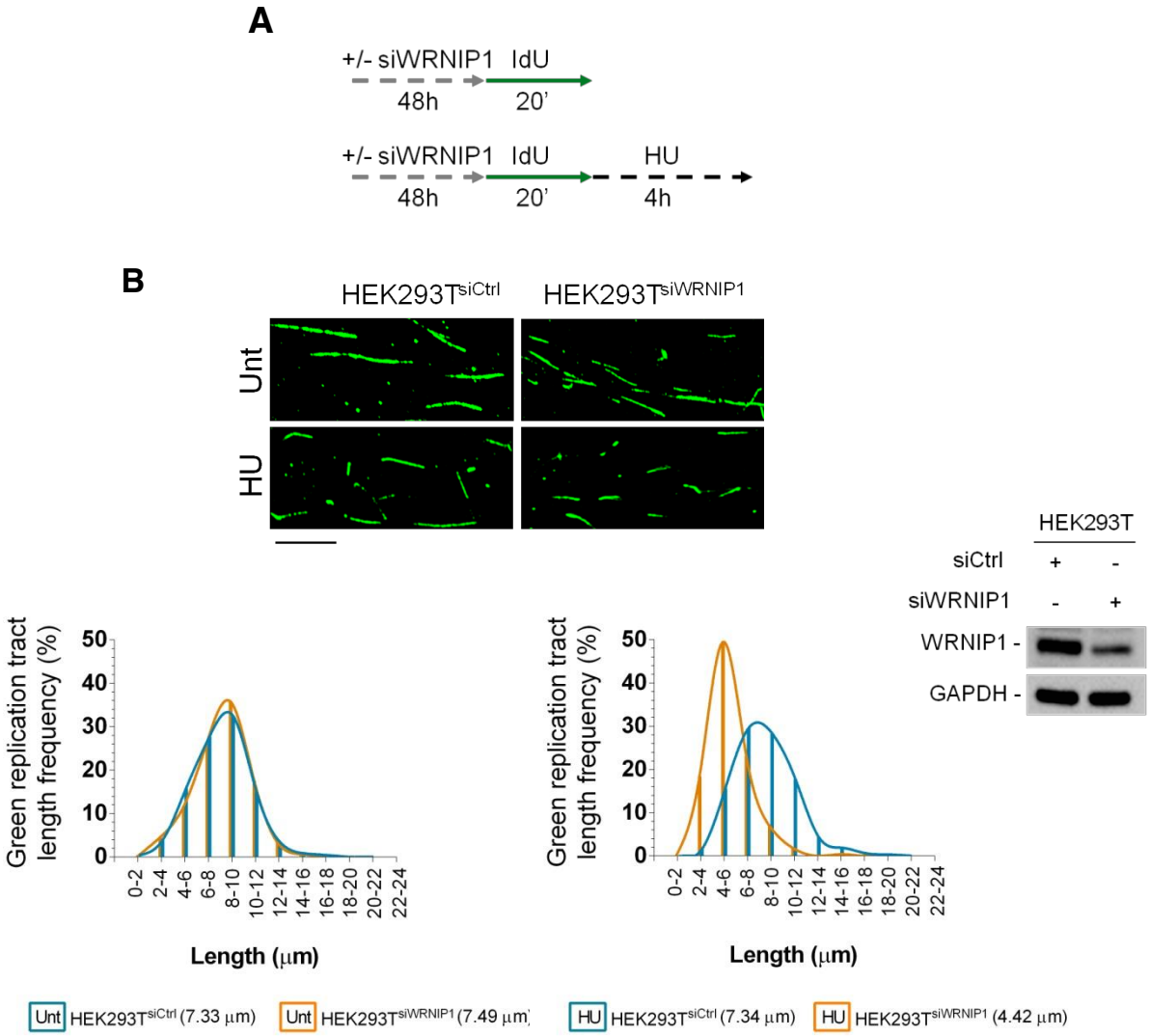

Appendix Figure S3

A

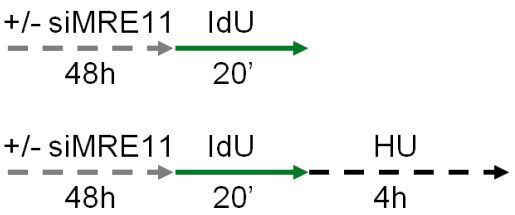

B

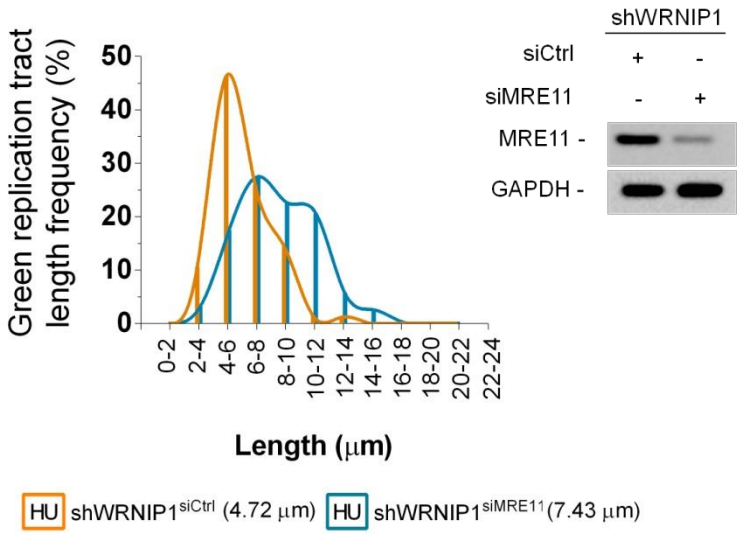

Appendix Figure S4

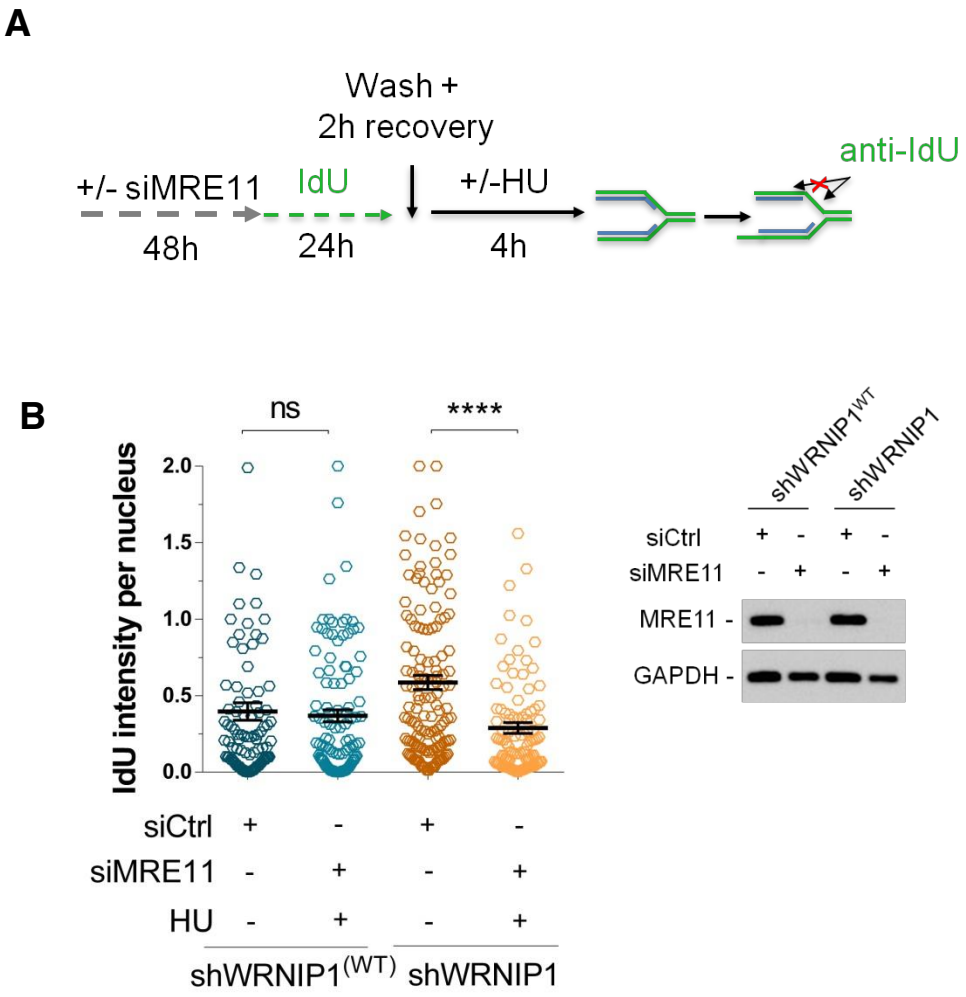

Appendix Figure S5

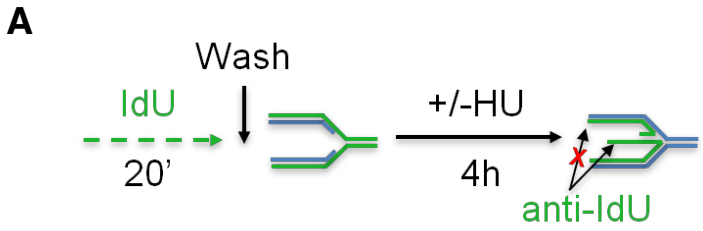

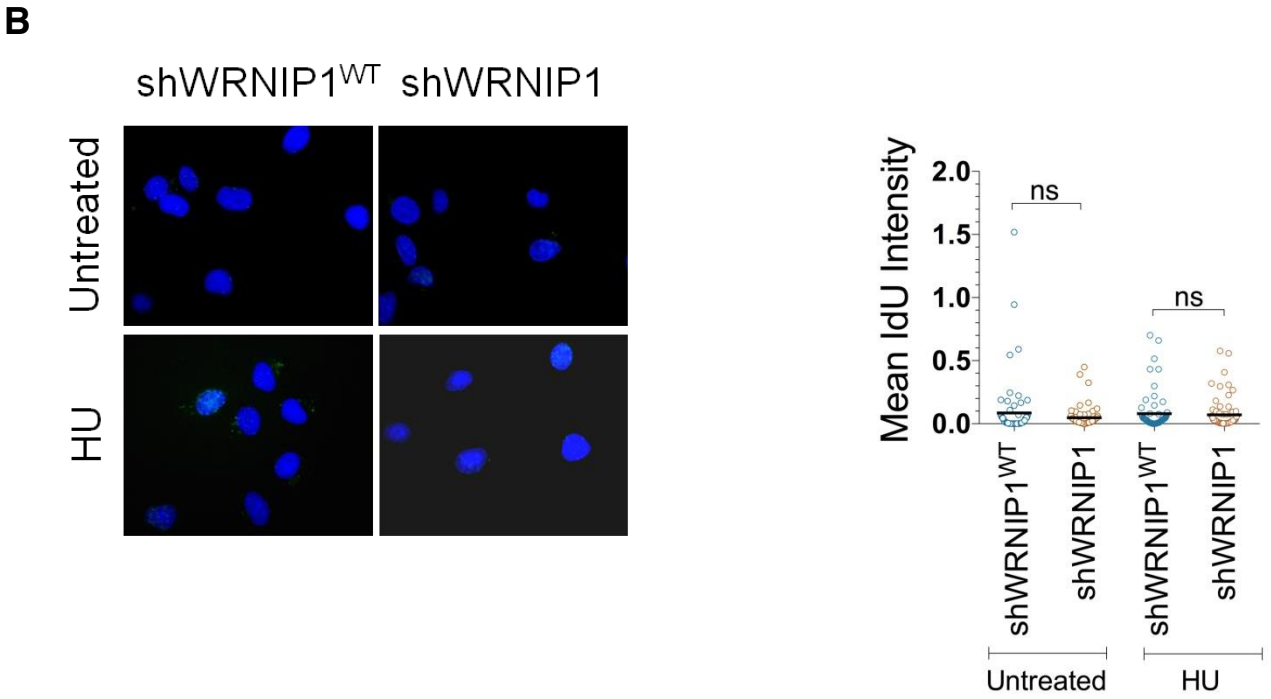

Appendix Figure S6

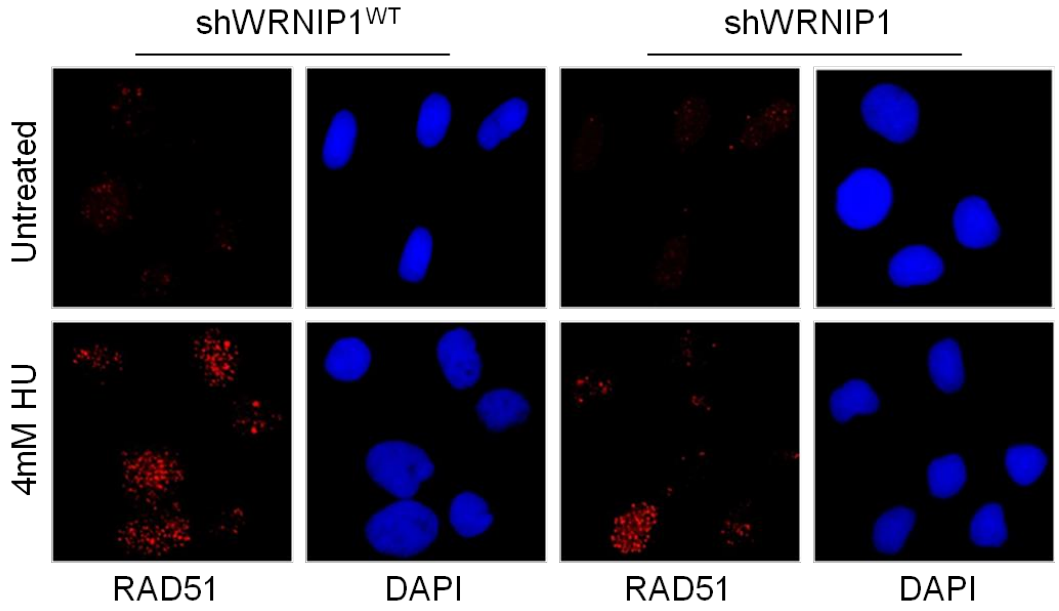

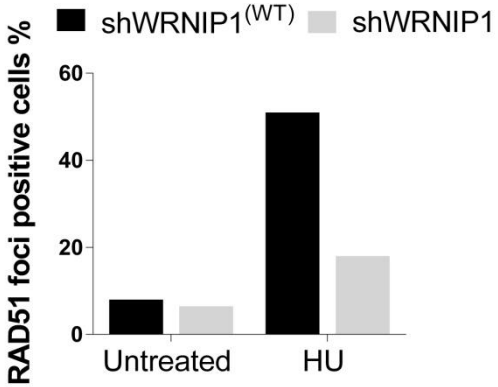

Appendix Figure S7

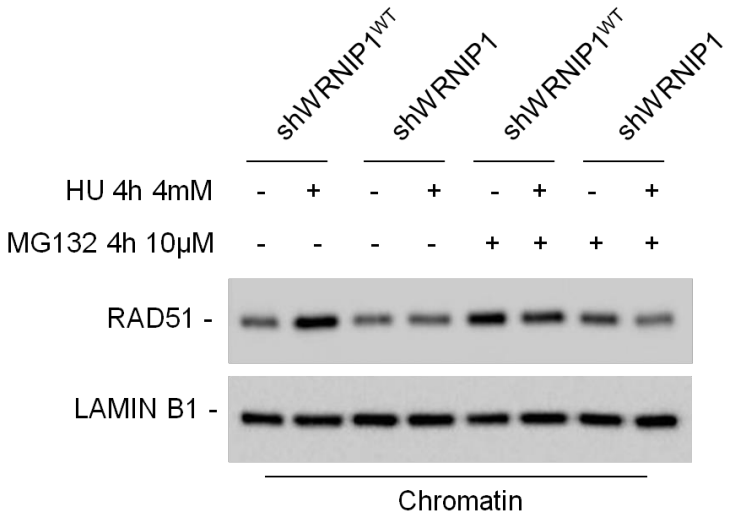

Appendix Figure S8

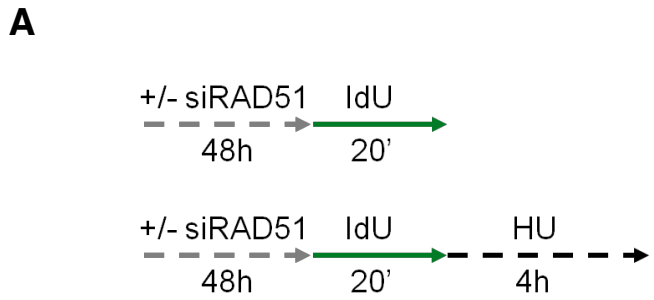

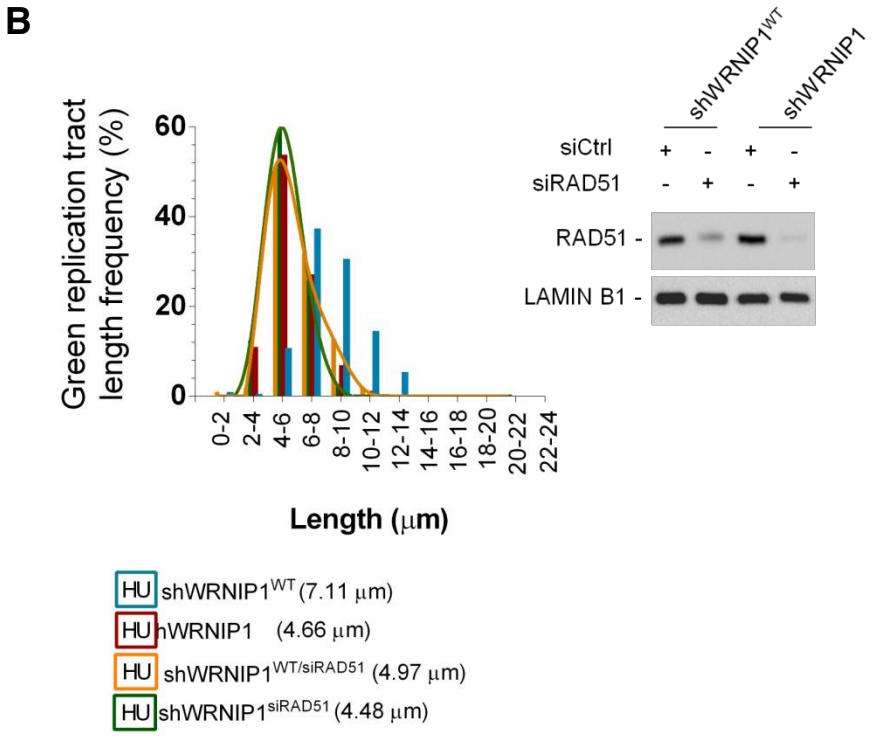

Appendix Figure S9

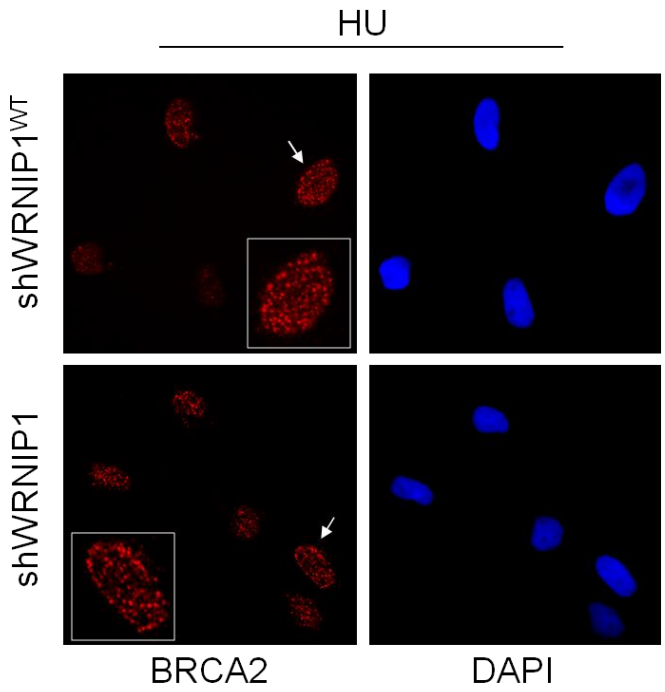

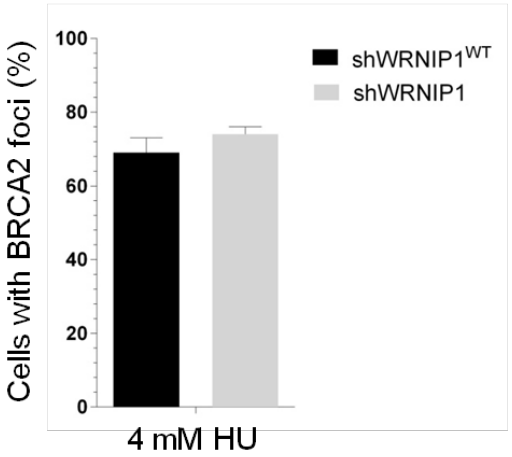

Appendix Figure S10

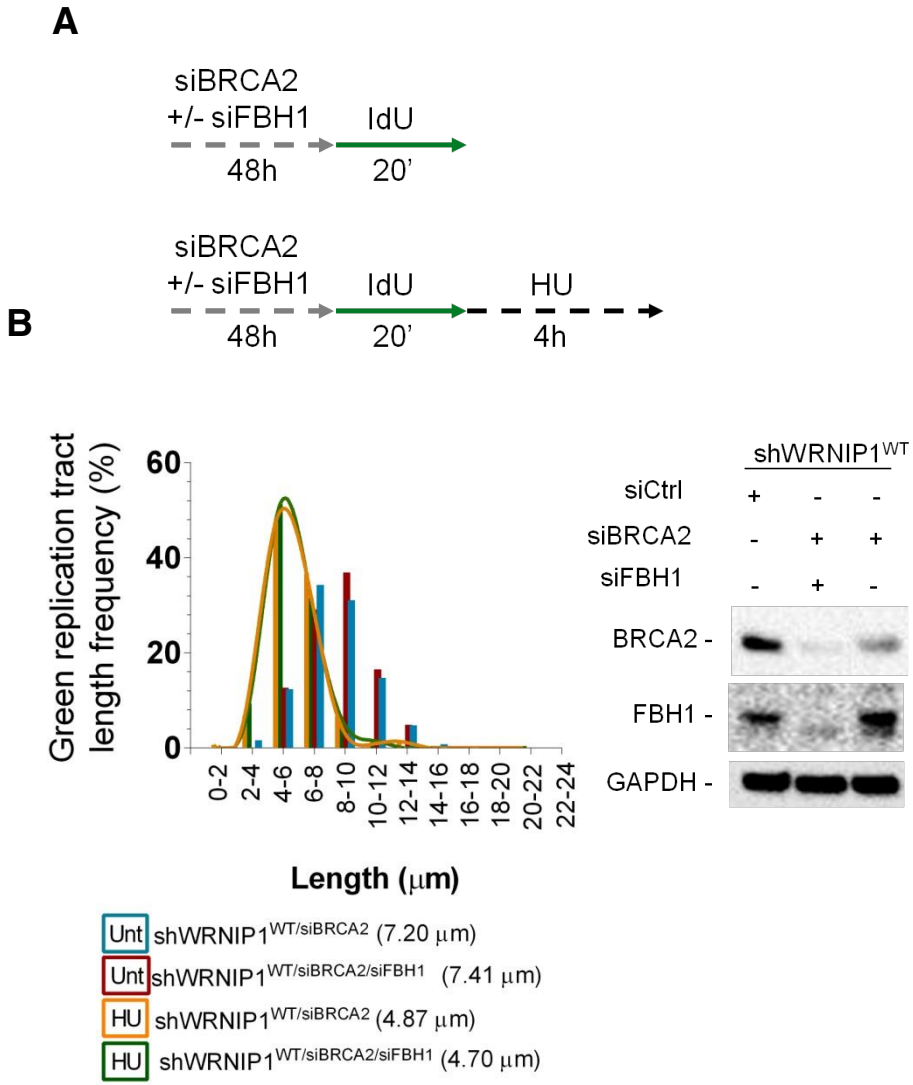

Appendix Figure S11

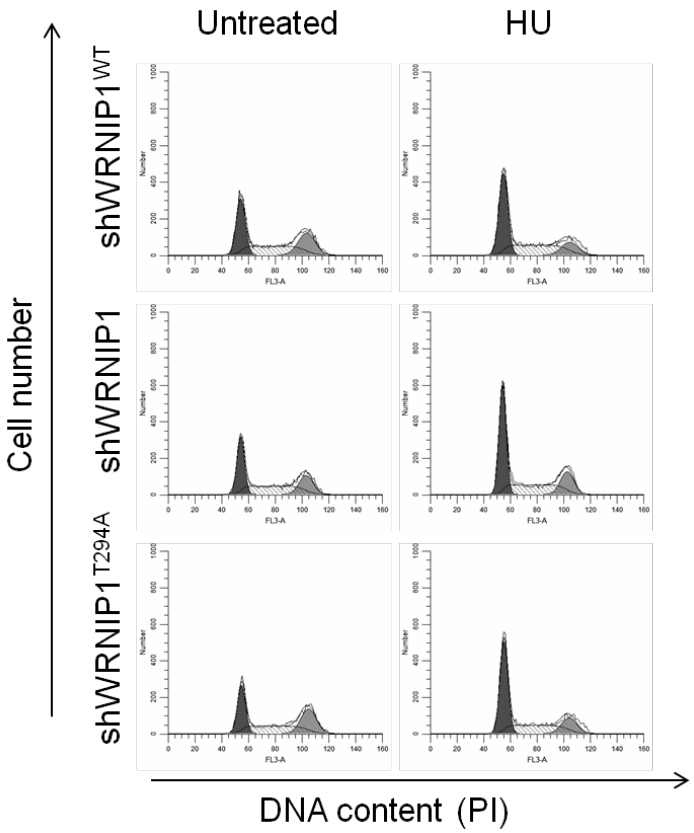

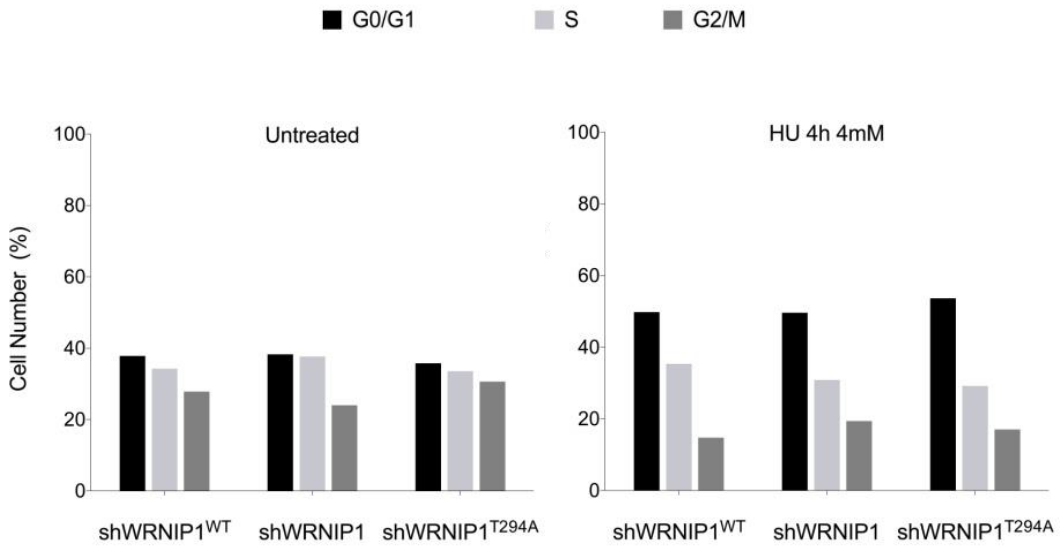

Appendix Figure S12

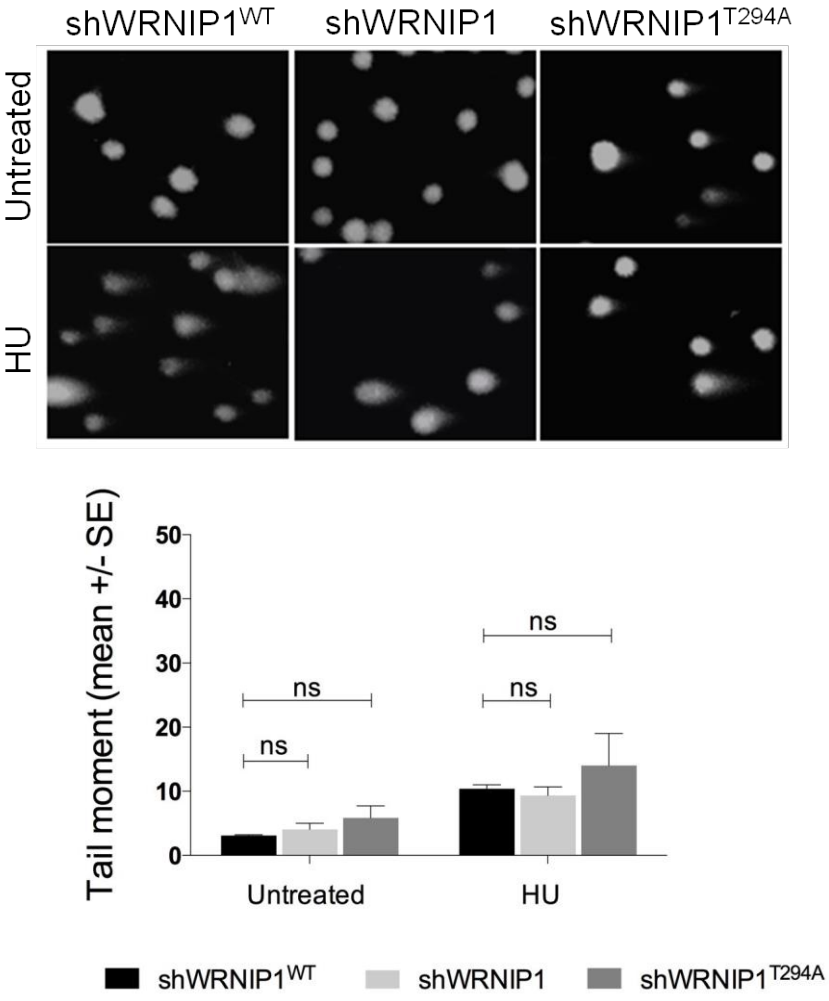

Appendix Figure S13

A

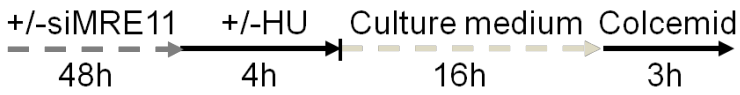

B

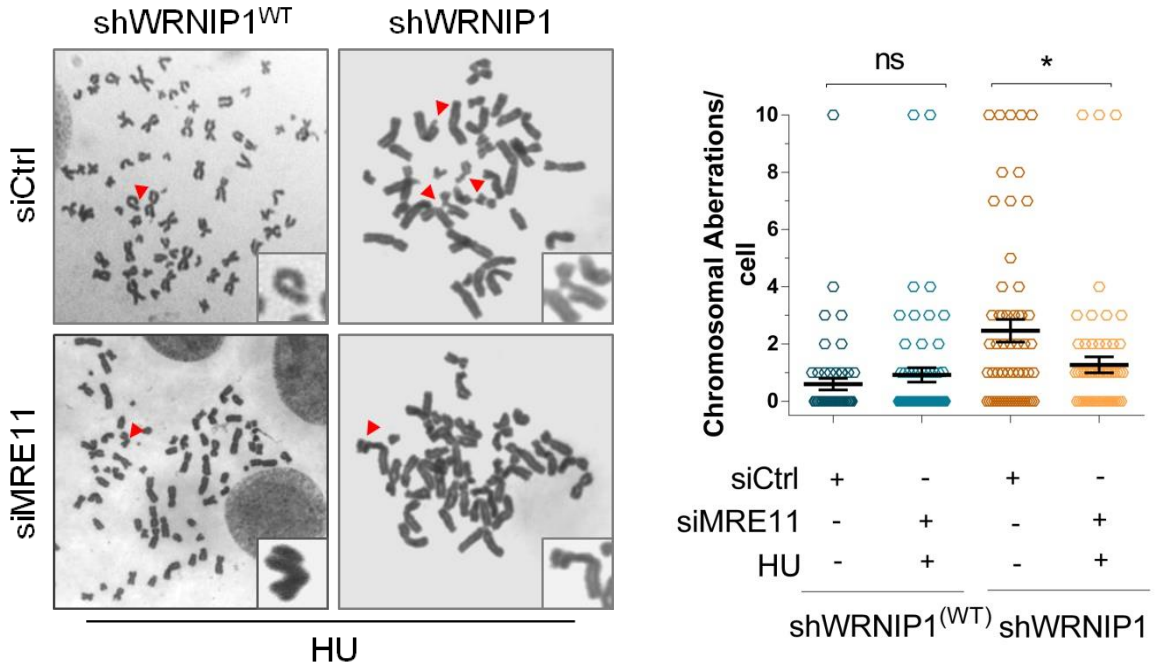

Appendix Figure S14

Appendix Table S1. Dataset and statistical information of DNA fibers spread

	Cell line	Treatment	Pulse-Labeling	Fiber analyzed	Median	* p-value (two-tailed)	* p-value (two-tailed)	Mean	SEM		Out of repeats	Total number of fibres	Link to Figures
1.	shWRNIP1^{WT}	HU	CldU-IdU	IdU	7.72	< 0.0001 vs 3.	0.8049 vs 2.	7.84	0.18		3	520	FIGURE 1 H
2.	shWRNIP1^{WT}	Untreated	CldU-IdU	IdU	7.96	0.0512 vs 4.		7.82	0.14		3	612	
3.	shWRNIP1	HU	CldU-IdU	IdU	4.70	< 0.0001 vs 5.	< 0.0001 vs 4.	4.90	0.09		3	590	
4.	shWRNIP1	Untreated	CldU-IdU	IdU	7.43	0.0899 vs 6.		7.47	0.15		3	450	
5.	shWRNIP1^{T294A}	HU	CldU-IdU	IdU	7.30	0.0672 vs 1.	0.5620 vs 6.	7.39	0.12		3	523	
6.	shWRNIP1^{T294A}	Untreated	CldU-IdU	IdU	7.40	0.0511 vs 2.		7.55	0.14		3	465	
7.	HEK293T ^{siCtrl}	HU	IdU	IdU	7.34		0.2766 vs 8.	7.48	0.15		2	481	
8.	HEK293T ^{siCtrl}	Untreated	IdU	IdU	7.33	0.253 vs 10.		7.12	0.16		2	385	FIGURE S3 B
9.	HEK293T ^{siWRNIP1}	HU	IdU	IdU	4.42	< 0.0001 vs 7.		4.60	0.10		2	538	
10.	HEK293T ^{siWRNIP1}	Untreated	IdU	IdU	7.49		< 0.0001 vs 9.	7.36	0.18		2	483	
11.	shWRNIP1^{WT}	HU	CldU-IdU	IdU	8.51		0.524 vs 12.	8.51	0.25		3	412	FIGURE 2 B
12.	shWRNIP1^{WT}	HU+Mirin	CldU-IdU	IdU	7.90	0.637 vs 14.		7.87	0.18		3	393	
13.	shWRNIP1	HU	CldU-IdU	IdU	4.95	< 0.0001 vs 11.		5.16	0.17		3	461	
14.	shWRNIP1	HU+Mirin	CldU-IdU	IdU	7.89		< 0.0001 vs 13.	7.61	0.17		3	412	
15.	shWRNIP1^{WT}	HU	IdU	IdU	7.40		0.381 vs 17.	7.77	0.15		3	620	FIGURE 4 B
16.	shWRNIP1^{WT}	Untreated	IdU	IdU	7.83	0.817 vs 20.	< 0.0001 vs 18.	7.91	0.16		3	513	
17.	shWRNIP1^{WT}	HU+RAD51i	IdU	IdU	5.72		< 0.0001 vs 16.	5.75	0.14		3	335	
18.	shWRNIP1	HU	IdU	IdU	5.31	< 0.0001 vs 16.	< 0.0001 vs 20.	5.45	0.07		3	1043	
19.	shWRNIP1	Untreated	IdU	IdU	7.77		< 0.0001 vs 21.	7.91	0.12		3	583	
20.	shWRNIP1	HU+RAD51i	IdU	IdU	5.36	0.329 vs 18.	0.275 vs 19.	5.67	0.13		3	629	
21.	shWRNIP1$^{TV-RAD51}$	HU	IdU	IdU	7.89			7.78	0.17		3	773	FIGURE 4 D
22.	shWRNIP1	HU	IdU	IdU	5.11	< 0.0001 vs 22.		5.27	0.11		3	863	
23.	shWRNIP1 ^{siMRE11}	HU	IdU	IdU	7.43			7.45	0.14		3	707	FIGURE S4
24.	shWRNIP1 ^{siCtrl}	HU	IdU	IdU	4.72	< 0.0001 vs 24.		5.14	0.10		3	816	
25.	shWRNIP1^{WT}	Aph	IdU	IdU	7.45	< 0.0001 vs 27.		7.76	0.15		3	1345	FIGURE S2
26.	shWRNIP1^{WT}	Untreated	IdU	IdU	7.52		0.927 vs 25.	7.67	0.13		3	1155	
27.	shWRNIP1	Aph	IdU	IdU	4.83		< 0.0001 vs 28.	5.28	0.10		3	1237	
28.	shWRNIP1	Untreated	IdU	IdU	7.34	0.0551 vs 25.		7.35	0.19		3	1123	
29.	shWRNIP1$^{WT\ siBRCA2}$	HU	IdU	IdU	4.67		< 0.0001 vs 30.	5.09	0.08		3	1054	FIGURE 5 D
30.	shWRNIP1$^{WT\ siBRCA2}$	Untreated	IdU	IdU	7.18	0.990 vs 32.		7.60	0.17		3	783	
31.	shWRNIP1 ^{siBRCA2}	HU	IdU	IdU	4.56	0.136 vs 29.		4.86	0.09		3	886	
32.	shWRNIP1 ^{siBRCA2}	Untreated	IdU	IdU	7.40		< 0.0001 vs 31.	7.65	0.18		3	1050	
33.	shWRNIP1 ^{siCtrl}	Untreated	IdU	IdU	8.72	0.887 vs 35.		8.79	0.14		2	623	FIGURE 5 F
34.	shWRNIP1 ^{siCtrl}	HU	IdU	IdU	4.76		< 0.0001 vs 33.	5.12	0.10		2	952	
35.	shWRNIP1 ^{siFBH1}	Untreated	IdU	IdU	8.69		0.463 vs 36.	8.71	0.14		2	677	
36.	shWRNIP1 ^{siFBH1}	HU	IdU	IdU	7.69	< 0.0001 vs 34.		7.92	0.13		2	936	
37.	shWRNIP1$^{WT\ siBRCA2}$	Untreated	IdU	IdU	7.20	0.5929 vs 39.					1	251	FIGURE S11
38.	shWRNIP1$^{WT\ siBRCA2}$	HU	IdU	IdU	4.87		< 0.0001 vs 37.				1	150	
39.	shWRNIP1$^{WT\ siBRCA2/siFBH1}$	Untreated	IdU	IdU	7.41		< 0.0001 vs 40.				1	103	
40.	shWRNIP1$^{WT\ siBRCA2/siFBH1}$	HU	IdU	IdU	4.70	0.2669 vs 38.					1	320	
41.	shWRNIP1^{WT}	HU	IdU	IdU	7.11	< 0.0001 vs 43.					1	110	FIGURE S9
42.	shWRNIP1$^{WT/siRAD51}$	HU	IdU	IdU	4.97		< 0.0001 vs 41.				1	206	
43.	shWRNIP1	HU	IdU	IdU	4.66		0.6122 vs 44.				1	173	
44.	shWRNIP1^{siRAD51}	HU	IdU	IdU	4.48	0.0511 vs 42.					1	101	

Medians and means are in µm. SEM, standard error of the mean. p-value derived from nonparametric test (Mann-Whitney test).

Appendix Table S2. DNA fibers lengths distributions data analysis information

	Cell line	Treatment	Pulse-Labeling	Fiber analyzed	IdU lengths distribution (in Percentage)											Link to Figures
					0	2	4	6	8	10	12	14	16	18	20	
1.	shWRNIP1^{WT}	HU	CldU-IdU	IdU	0	1,27	8,23	**28,48**	**31,65**	21,52	6,96	1,9	0	0	0	FIGURE 1 H
2.	shWRNIP1^{WT}	Untreated	CldU-IdU	IdU	0,4	0,4	9,13	**28,17**	**34,13**	19,84	7,14	0,79	0	0	0	
3.	shWRNIP1	HU	CldU-IdU	IdU	0	11,26	**44,71**	**33,79**	7,85	2,05	0,34	0	0	0	0	
4.	shWRNIP1	Untreated	CldU-IdU	IdU	0,37	2,21	12,55	**27,68**	**33,58**	16,97	4,06	1,85	0,74	0	0	
5.	shWRNIP1^{T294A}	HU	CldU-IdU	IdU	0	0,47	7,01	**36,92**	**37,38**	13,55	4,21	0,47	0	0	0	
6.	shWRNIP1^{T294A}	Untreated	CldU-IdU	IdU	0	1,16	8,88	**35,91**	**33,59**	12,74	5,02	2,32	0,39	0	0	
7.	HEK293T ^{siCtrl}	HU	IdU	IdU	0	1,25	14,64	**29,6**	**28,97**	17,13	4,98	2,49	0,62	0,31	0	FIGURE S3 B
8.	HEK293T ^{siCtrl}	Untreated	IdU	IdU	0,43	3,85	14,53	**28,21**	**32,48**	15,81	3,42	0,85	0,43	0	0	
9.	HEK293T ^{siWRNIP1}	HU	IdU	IdU	0	16,97	**49,46**	**23,47**	7,58	2,17	0	0,36	0	0	0	
10.	HEK293T ^{siWRNIP1}	Untreated	IdU	IdU	0	3,25	11,69	**25,97**	**37,01**	18,18	2,6	1,3	0	0	0	
11.	shWRNIP1^{WT}	HU	CldU-IdU	IdU	0	0	10,61	**21,97**	**41,67**	**18,94**	6,06	0	0,76	0	0	FIGURE 2 B
12.	shWRNIP1^{WT}	HU+Mirin	CldU-IdU	IdU	0	1,63	8,13	**18,7**	**28,46**	**26,83**	9,76	4,07	2,44	0	0	
13.	shWRNIP1	HU	CldU-IdU	IdU	0	13,11	**38,52**	**33,61**	**10,66**	3,28	0	0,82	0	0	0	
14.	shWRNIP1	HU+Mirin	CldU-IdU	IdU	0	1,16	11,63	**26,16**	**31,4**	**25**	2,91	1,74	0	0	0	
15.	shWRNIP1^{WT}	HU	IdU	IdU	0	0	13,91	**29,7**	**27,82**	**17,29**	7,89	2,26	1,13	0	0	FIGURE 4 B
16.	shWRNIP1^{WT}	Untreated	IdU	IdU	0	0,45	11,31	**24,89**	**33,03**	**20,36**	6,33	2,71	0,9	0	0	
17.	shWRNIP1^{WT}	HU+RAD51i	IdU	IdU	0,68	3,42	**33,56**	**35,62**	**23,29**	3,42	0	0	0	0	0	
18.	shWRNIP1	HU	IdU	IdU	0,36	6,08	**38,46**	**36,14**	**14,31**	4,11	0,54	0	0	0	0	
19.	shWRNIP1	Untreated	IdU	IdU	0	1,13	7,61	**29,3**	**30,14**	**21,41**	9,01	1,41	0	0	0	
20.	shWRNIP1	HU+RAD51i	IdU	IdU	0,65	7,82	**33,55**	**31,6**	**18,89**	4,89	2,61	0	0	0	0	
21.	shWRNIP1$^{TV-RAD51}$	HU	IdU	IdU	0	1,26	14,29	**18,91**	**37,39**	16,81	7,56	2,94	0,42	0,42	0	FIGURE 4 D
22.	shWRNIP1	HU	IdU	IdU	0	5,23	**42,86**	**31,01**	15,68	4,53	0,7	0	0	0	0	
23.	shWRNIP1 ^{siMRE11}	HU	IdU	IdU	0	2,87	16,91	**28,08**	**20,92**	22,64	5,73	2,58	0,29	0	0	FIGURE S4
24.	shWRNIP1 ^{siCtrl}	HU	IdU	IdU	0	9,73	**45,72**	**26,25**	15,34	1,77	1,18	0	0	0	0	
25.	shWRNIP1^{WT}	Aph	IdU	IdU	0	3,63	15,98	**23,97**	**26,63**	16,46	7,75	2,18	2,91	0,24	0	FIGURE S2
26.	shWRNIP1^{WT}	Untreated	IdU	IdU	0	1,01	13,67	**28,61**	**30,89**	14,94	7,34	2,53	0,76	0,25	0	
27.	shWRNIP1	Aph	IdU	IdU	0	15,74	**37,56**	**26,73**	12,52	3,89	1,86	1,18	0	0	0,17	
28.	shWRNIP1	Untreated	IdU	IdU	0	2,42	19,38	**25,95**	**27,68**	12,46	7,96	2,77	1,04	0,35	0	
29.	shWRNIP1$^{WT\ siBRCA2}$	HU	IdU	IdU	0	12,54	**44,13**	**27,62**	10,32	3,65	1,11	0,48	0,16	0	0	FIGURE 5 D
30.	shWRNIP1$^{WT\ siBRCA2}$	Untreated	IdU	IdU	0	2,13	16,41	**29,18**	**24,92**	16,72	5,47	2,43	1,52	0,91	0	
31.	shWRNIP1 ^{siBRCA2}	HU	IdU	IdU	0	15,76	**43,6**	**28,57**	6,65	4,68	0,74	0	0	0	0	
32.	shWRNIP1 ^{siBRCA2}	Untreated	IdU	IdU	0	2,42	20,85	**24,17**	**22,66**	15,11	8,76	3,93	0,91	0,91	0,3	
33.	shWRNIP1 ^{siCtrl}	Untreated	IdU	IdU	0	0	7.77	**20.27**	**27.50**	**24.44**	14.17	4.17	1.11	0.28	0.27	FIGURE 5 F
34.	shWRNIP1 ^{siCtrl}	HU	IdU	IdU	0.26	**15.10**	**41.14**	**27.60**	10.67	4.68	0.52	0	0	0	0	
35.	shWRNIP1 ^{siFBH1}	Untreated	IdU	IdU	0	0.84	8.45	**18.30**	**29.29**	**26.19**	12.39	2.81	1.40	0.28	0	
36.	shWRNIP1 ^{siFBH1}	HU	IdU	IdU	0.49	1.74	12.18	**29.10**	**27.36**	**16.91**	7.71	2.98	0.99	0.49	0	
37.	shWRNIP1$^{WT\ siBRCA2}$	Untreated	IdU	IdU	0	1.59	12.35	**34.26**	**31.07**	**14.74**	4.78	0.79	0.39	0	0	FIGURE S11
38.	shWRNIP1$^{WT\ siBRCA2}$	HU	IdU	IdU	0.66	6.66	**47.33**	**36.66**	6.66	0.66	1.33	0	0	0	0	
39.	shWRNIP1$^{WT\ siBRCA2/siFBH1}$	Untreated	IdU	IdU	0	0	12.62	**29.12**	**36.89**	**16.50**	4.85	0	0	0	0	
40.	shWRNIP1$^{WT\ siBRCA2/siFBH1}$	HU	IdU	IdU	0.31	**9.37**	**51.25**	**31.56**	5.93	1.56	0	0	0	0	0	
41.	shWRNIP1^{WT}	HU	IdU	IdU	0.97	0.48	10.67	**37.37**	**30.58**	**14.56**	5.33	0	0	0	0	FIGURE S9
42.	shWRNIP1$^{WT/siRAD51}$	HU	IdU	IdU	0.90	1.81	**50.90**	**31.81**	**12.72**	1.81	0	0	0	0	0	
43.	shWRNIP1	HU	IdU	IdU	0	10.98	**53.75**	**27.16**	**6.90**	1.15	0	0	0	0	0	
44.	shWRNIP1^{siRAD51}	HU	IdU	IdU	0	12.35	**59.95**	**25.85**	**2.24**	0	0	0	0	0	0	

IdU lengths are in µm. Distributions are in percentage. Red values represent the dominant rate of distribution.